ELSEVIER

Biochimica et Biophysica Acta 1234 (1995) 5–14

BBA Biochimica et Biophysica Acta

Active transport of ions across membranes: energetic role of electrostatics and binding site asymmetry

Ming-Hong Hao [1], Stephen C. Harvey *

Department of Biochemistry and Molecular Genetics, University of Alabama at Birmingham, Birmingham, AL 35294-0005, USA

Received 22 September 1994; accepted 2 November 1994

Abstract

The active transport of ions across a membrane by an ATP-driven electrogenic ion pump is often described by an 'alternate access' model. The position of the binding site is assumed to be unchanged as the binding cavity opens alternatively to the uptake and discharge sides of the membrane. The ion binding affinity is higher on the uptake side of the membrane than on the discharge side. This difference in affinities is related to the maximum transport rate and to the efficiency with which ATP hydrolysis is coupled to active transport. Here we examine the electrostatic contribution to binding affinities, using a simple geometry for a model membrane-protein system, a continuum dielectric approximation, and a numerical method to calculate binding energy as a function of the binding site location. If the binding site is located asymmetrically, being further from the uptake side of the membrane than from the discharge side, there is a significant difference in binding free energy between the uptake and discharge states. This asymmetry can produce differences in affinities that are consistent with those measured for biological active transport systems. These results may account for the observed asymmetric location of the calcium binding site in the calcium ATPases from sarcoplasmic reticulum and from the plasma membrane. Electrostatic energy differences associated with binding site asymmetry may be a general feature of electrogenic transmembrane ion pumps.

Keywords: Ion transport; Active transport; Electrostatics; ATPase, Ca^{2+}-; Binding site asymmetry

1. Introduction

There are a number of specialized proteins for the movement of ions across membranes [1–3]. Using ATP as an energy source, these systems can actively transport ions against concentration gradients as high as three or four orders of magnitude. Alternatively, they can extract the energy available in the chemical potential by coupling the downhill transfer of ions to the synthesis of ATP. It is obviously important to understand the mechanism by which conformational changes in these proteins convert the energy released by ATP hydrolysis to the increased free energy of the transported ions [3,4].

Active transport processes have two essential features: directionality and efficiency. In order for ions to move only in the desired direction, the system must accept ions from one side of the membrane and release them on another side. Experiments have shown that the binding site has a higher ion binding affinity on the uptake side of the membrane, and a lower affinity on the discharge side [4]. Theoretical treatments show that such differences are related to the maximum transport rate [3,5,6]. For maximum efficiency, the affinity difference for ion binding to the uptake and discharge conformations should match the chemical potential difference due to the concentration difference of the ions on the two sides of the membrane [6]. Any theoretical model for ion active transport has to take account of these features.

In the earliest model for active transport [7–9], the directionality of ion movement is controlled by the alternative opening of a binding cavity to different sides of membrane for the uptake and release of ions. The difference in binding affinity at the uptake and release states was not explicitly specified in the original theory. A more refined model was proposed later by Tanford [6]. In this model, the accessibility of the binding site to ions on different sides of membrane is coupled to specific conformational changes in the transport protein. In the uptake

* Corresponding author. E-mail: harvey@neptune.cmc.uab.edu. Fax: +1 (205) 9752547.

[1] Present address: Department of Chemistry, Baker Laboratory, Cornell University, Ithaca, NY 14853-1301, USA.

SSDI 0005-2736(94)00265-7

conformation, it is assumed that there are more negatively charged groups near the binding site to provide a high binding affinity for positive ions, and the site is only accessible to the side of low ion concentration. At the discharge stage, conformational changes in the protein change the accessibility of the binding site from the uptake side to the discharge side; simultaneously, some of the negatively charged groups move away from the binding site, weakening the binding affinity. In all these models [6–9], the binding site is located in the transmembrane region, and energy to drive the cycle is derived from the hydrolysis of ATP.

The main purpose of the present study is to explore the effects of electrostatic interactions on ion active transport, investigating how they would affect association constants if the binding site were asymmetrically located with respect to the openings of the entrance and exit channels. It is not possible to calculate the exact ion binding constants to the transport proteins, because the detailed molecular structure of the system is still unknown. However, the electrostatic interaction energies between free charges and dielectric media can be estimated with a few simple assumptions. We find that the results of these calculations are only weakly dependent on the detailed model for the molecular structure.

The protein-membrane interior can be modeled as a low dielectric medium, with a dielectric constant of about 2 to 4 [10,11]. The bulk water is a high dielectric medium with dielectric constant 80. Earlier theoretical studies on ion transport have successfully modeled ion channels as aqueous pores through a low dielectric medium [12–14]. We have consequently modeled the ion binding site as a charged ring in the bottom of a high dielectric aqueous cavity, surrounded by aqueous and membrane-protein phases. Our objective is to estimate the polarization energy of the dielectric media under the influence of these charges in the uptake and release conformations. The energy difference between these two states explains the difference in binding affinities of the two conformations, since ion binding neutralizes the protein charged groups at the binding site and eliminates the polarization charges.

As reviewed by Läuger [3], there are two extreme classes of models for active transport. At one extreme are those where the electrical conductance of the access channel is large, so the field strength resulting from the transmembrane voltage is low. These models are therefore called *low field models*. At the other extreme are *high field models*, in which the field strength is high, because the voltage drops along the length of the channel. Models where the solvent in the channel is assumed to have the dielectric and conductance properties of water at physiological ionic strength will be low field models if the channel is sufficiently wide. If the access channel is very narrow, however, the conductance will necessarily be low, and the model will fall into the high field class. There is experimental evidence for the existence of access channels of the high field class [15–17]; see Läuger [3] for a complete review). As will be seen, our model falls between these two extremes.

We are particularly motivated by the observation that the location of the ion binding site with respect to the two sides of membrane may be quite asymmetric. First, the earlier theoretical models [6,9] and more recent experiments [18–21] have suggested that the binding sites in ion pumps for active ion transport are located in the transmembrane domain. Second, electron microscopic investigations show that the sarcoplasmic reticulum (SR) and plasma membrane calcium ATPases embed in the membrane in a very asymmetric manner [1,19,22]. A large portion of the protein, the stalk domain, protrudes into the solvent on the side of low ionic strength. Site-specific mutagenesis experiments on the SR calcium ATPase [18,20] show that changing charged residues to neutral residues in the stalk domain of the protein does not significantly affect the ability of the ATPase in transporting calcium ion, while the mutation of charged residues to neutral residues in the transmembrane region almost eliminates the transport of the cation. Therefore, it appears likely that the binding site for ion active transport is located in the transmembrane region rather than in the stalk domain, even though the latter is known to have a high affinity for binding cations [20,21]. Although the exact geometry of the channel is not known, the overall structure suggests that the binding site could be substantially further from the protein/solvent interface on the uptake side than it is from the discharge side. It is then relevant to examine the energetics of electrostatic interactions in an asymmetric system and to investigate the possible contributions of these interactions to active transport.

2. Theory

2.1. The contribution of polarization energy to ion binding

We base our initial calculations on the simple model shown in Fig. 1. The membrane-protein system is an infinite slab of thickness H. The binding cavity is assumed to be a cylindrical well of radius r. The charged groups of the protein that bind the ion are modeled as a ring of charge, located 1 Å above the bottom of the well, and the bound ion is assumed to sit in the center of this ring. If the bound ion has charge q, then the total charge on the ring is $-q$. In analogy to the alternative access model of ion active transport [6], the conformational change of the protein is assumed to change the access of the binding site to the two sides of the membrane. In contrast with that model, however, we assume that the positions of the charges (ion and charged groups on the protein) do not vary during the conformational change. Conformations (a) and (b) in Fig. 1 correspond to the E_1 and E_2 states of the ATPase, respectively.

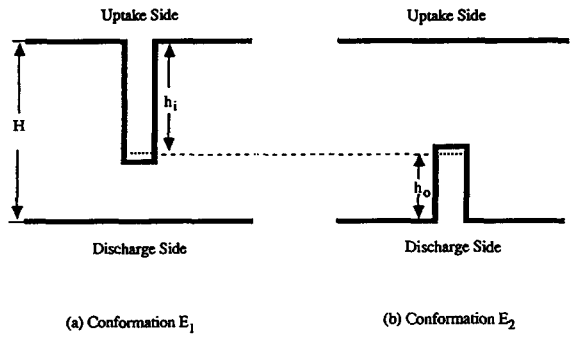

Fig. 1. Schematic of the alternative access model for transport, showing (a) conformation E_1 for ion uptake; (b) conformation E_2 for ion release. The dashed line indicates the ring charge lining the binding site. H is the total thickness of the membrane, while h_i and h_o are the depths of the binding wells in the two conformational states.

While this model is clearly an oversimplification, it is intended to provide a clean determination of the contributions of binding site asymmetry to the electrostatic component of the binding energies. We have examined the consequences of varying the shape of the protein to more accurately reflect current structural knowledge, finding little effect on the results (see below).

The polarization energy depends on the geometry of the binding cavity, especially on the depth of the well. We denote the binding constant in the uptake state as K_1, and that of the discharge state as K_2. The contributions of the polarization energy to the binding constants in the two states can be separated from other contributions in the following form:

$$\ln\left(\frac{K_2}{K_1}\right) = \ln\left(\frac{K_{out}}{K_{in}}\right) - \frac{\Delta\Delta w}{RT} \quad (1)$$

where K_{in} and K_{out} are the binding constants of the two states when the polarization effects are imaginarily turned off, and $\Delta\Delta w$ is the difference of polarization energies between the two states. We write

$$\Delta\Delta w = \Delta w_{out} - \Delta w_{in} \quad (2)$$

where Δw is the polarization energy in one conformation. The primary task is to evaluate the contribution of Δw to the ion binding in a given conformation.

The polarization energy can be obtained from a macroscopic treatment of the electrostatics in macromolecular systems [23,24]. The electrostatic potential of the whole system is solved under a given set of boundary conditions. From this total potential, the potential due to the permanent charges in the reference homogeneous medium should be subtracted. The remaining part is the polarization potential. To obtain the polarization energy, one may apply a continuous charging process. Assuming that the polarization of the dielectric medium has a linear response to the electric field, then the polarization energy is found to be

$$w = (1/2)\sum_i q_i \psi_p(r_i),$$

where the sum is over all permanent charges q_i involved in the system, and $\psi_p(r_i)$ is the polarization potential at the position of i^{th} charge. In order to obtain the contribution of the polarization energy to the binding energy of ions in the protein, the polarization potential should be solved twice: once without the ion, and another time with the ion. The difference between the polarization energies of the two cases is the polarization contribution to the binding free energy, denoted Δw.

The solution to the general boundary-value problem in electrostatics is a nontrivial task. Numerical solutions to the Poisson-Boltzmann equation, using the usual finite difference method [25–27] or the more recently developed finite element approach [28] would require detailed knowledge of the geometry of the protein and the channel, along with the locations of all charges. At present, such knowledge is not available, so we have introduced the simple geometry described above.

Since even this geometry is too complex for analytical solution, we have calculated the polarization energy using the image potential method [13,23]. This method is based on the recognition that the boundary value problem of electrostatics in a heterogeneous system can be mimicked by a homogeneous system with an appropriate surface charge density (image charge) distributed on the interfaces between the different dielectric media. Once these image charge densities are obtained, the polarization energy is simply one half of the interaction energy of the permanent charges with the image charges. This energy term can be directly calculated according to Coulomb's law, because the simulated system is homogeneous. The contribution of the polarization energy to ion binding may be conveniently calculated based on the additive property of the electrostatic potential: let q_1 be the charge of the bound ion, q_i ($i = 2$ to m) the charges of protein groups that bind the ion, ψ_{p1} the polarization potential of q_1, and ψ_{p2} the polarization potential of protein charged groups. Then

$$\Delta w = (1/2)q_1\left(\psi_{p1}(r_1) + \psi_{p2}(r_1)\right) + (1/2)\sum_i q_i\psi_{p1}(r_i) \quad (3)$$

The interaction energy of the protein charged groups with their own polarization potential, $\sum_i q_i\psi_{p1}(r_i)/2$, does not contribute to the binding energy of the ion to the protein or to differences in the ion binding affinity in the uptake and discharge states. The energy calculated in Eq. (3) represents the work that would be done on bringing the ion into the binding site from the aqueous medium at an infinite distance from the membrane. Binding constants can be calculated from this energy.

2.2. The polarization potential

There are two cases to consider: (a) the whole system consists of only two dielectric phases: the aqueous phase

and the membrane-protein phase, and the dielectric constant inside the binding cavity is identical to that of aqueous phase. (b) The dielectric constant inside the binding cavity is different from either of the other two phases, and there are three different dielectric media in the system. Case (a) would be a proper approximation. However, considering that the binding cavity is quite narrow in general, and that water molecules inside the well will be subjected to certain constraints, the dielectric constant inside the well may be somewhat lower than that of bulk water. In any rate, case (a) is simply a special case of case (b).

Let the dielectric constants of aqueous phase (denoted a), of the interior of protein and membrane (m), and of the binding cavity (c) be ϵ_a, ϵ_m and ϵ_c, respectively. The boundary conditions at the interfaces of these three dielectric media are

$$\psi_a(s_a) = \psi_m(s_m);\ \psi_a(s_a) = \psi_c(s_c);\ \psi_c(s_c) = \psi_m(s_m) \tag{4a}$$

$$\epsilon_a E_n(s_a) = \epsilon_m E_n(s_m);\ \epsilon_a E_n(s_a) = \epsilon_c E_n(s_c);$$
$$\epsilon_c E_n(s_c) = \epsilon_m E_n(s_m) \tag{4b}$$

where s represents a point on the interface, s_ξ (ξ = a, m, c) indicates the side of the surface that faces the x phase, ϕ is the total electrostatic potential, and E_n is the electrostatic field normal to the interface. All permanent charges are assumed to be located inside the binding cavity. Then the Poisson equations for this system are

$$\Delta^2\psi(\boldsymbol{r}) = -1/(2\pi\epsilon_c)\sum q_i\delta(\boldsymbol{r}-\boldsymbol{r}_i)\ \text{(binding cavity)} \tag{5a}$$

$$\Delta^2\psi(\boldsymbol{r}) = 0\ \text{(membrane phase)} \tag{5b}$$

$$\Delta^2\psi(\boldsymbol{r}) = 0\ \text{(aqueous cavity)} \tag{5c}$$

where ψ is the total electrostatic potential in the designated phase, $\delta(\boldsymbol{r})$ is the Dirac δ-function, and $\boldsymbol{r}_i$ is the position of the i^{th} permanent charge. This system of differential equations together with the boundary conditions can be simulated by a homogeneous system with dielectric constant ϵ_c (because the permanent charges are in the binding cavity). The required surface charge density $\sigma(s)$ can be deduced from the boundary conditions. We obtain:

$$\sigma_{ma}(s) = \frac{\epsilon_c}{2\pi}\frac{(\epsilon_a-\epsilon_m)}{(\epsilon_a+\epsilon_m)}E_n(s) \tag{6a}$$

$$\sigma_{cm}(s) = \frac{\epsilon_c}{2\pi}\frac{(\epsilon_a-\epsilon_c)}{(\epsilon_a+\epsilon_m)}E_n(s) \tag{6b}$$

$$\sigma_{ca}(s) = \frac{\epsilon_c}{2\pi}\frac{(\epsilon_a-\epsilon_c)}{(\epsilon_a+\epsilon_c)}E_n(s) \tag{6c}$$

where the subscripts to σ indicate the two phases that are in contact. The normal electric field $E_n(s)$ at point s on the interface can be expressed a function of the permanent charge and the surface charge density σ:

$$E_n(s) = \boldsymbol{n}\left\{\sum_i \frac{q_i(\boldsymbol{r}(s)-\boldsymbol{r}(q_i))}{\epsilon_c|\boldsymbol{r}(s)-\boldsymbol{r}(q_i)|^3} + \frac{1}{\epsilon_c}\int\frac{\sigma(s')[\boldsymbol{r}(s)-\boldsymbol{r}(s')]}{|\boldsymbol{r}(s')-r(s)|^3}ds'\right\} \tag{7}$$

where $\boldsymbol{n}$ is the outward normal vector to the surface at point s, and the integration is over all interfaces (ma, mc and ca). Eqs. (6) and (7) constitute a pair of coupled integral equations, from which the surface charge density can be determined. After $\sigma(s)$ is obtained, the polarization potential ψ_p at position $\boldsymbol{r}$ is simply calculated according to Coulomb's law, since the system is now a homogeneous one:

$$\psi_p(\boldsymbol{r}) = \frac{1}{\epsilon_c}\int\frac{\sigma(s)}{|\boldsymbol{r}(s)-\boldsymbol{r}|}ds \tag{8}$$

where the integration is over all interfaces. There will be also a self-energy term (the Born energy) for the charges in the binding cavity when the cavity has a different dielectric constant from that of water. However, in what follows we are concerned with the difference of two binding states, which are assumed to have similar dielectric properties. Then the self-energy terms do not enter into the difference between the two conformations, so we will not bother with them.

If the dielectric constant of the binding cavity is identical to that of bulk water, Eq. (6c) disappears, Eq. (6b) is equal to Eq. (6a), and the other equations that describe such systems are formally identical to those shown above.

2.3. Numerical calculations

The interface charge density is solved here by an iteration method. From initially guessed values, the charge density is obtained by repeatedly using Eqs. (6) and (7) until the charge density converges to the correct value. The 'averaging function corrections' method [29] used by Levitt [13] is particularly effective in achieving convergence in the calculations. The numerical procedure is very similar to that used by Levitt to solve the energy barrier for the transport of ions across a membrane. In the present problem, the interfaces have complicated geometries and there are more phases, so there are more interaction terms.

To simplify the computation, the charges of protein groups which directly bind to the ion are considered to be distributed on a circular ring in the membrane phase, located 1 Å above the bottom of the cylindrical cavity and 0.5 Å away from the side wall of the cavity. The total charge on the ring is equal in magnitude, but of opposite sign, to the charge of the bound ion. This guarantees electrostatic neutrality. The bound ion is placed at the center of the ring, so that the system has cylindrical

symmetry. Because of this symmetry, the analysis reduces to a one-dimensional problem. We need only find the charge density $\sigma(x)$ along a path x leading from the center of the bottom of the well, radially outward to the side of the well, then up the side of the well to the surface of the membrane, then radially outward away from the well. To perform the numerical integration, the bottom surface of the well is divided radially into 0.3 Å steps, the side surface of the well is divided into 1 Å steps, and the upper and lower surfaces of the membrane-protein are divided first into 0.5 Å steps for 10 steps, then into 1 Å steps for 10 steps, followed 8 Å steps for 20 steps. The effects of interfaces further from the cavity are negligible. We did not make the singularity correction to the polarization potential at the corners of the interfaces as suggested by Jordan [14]. The corrections due to corners are generally small, and, considering the crudity of our model, the additional computational complexity is unwarranted. Test calculations of the program on an open channel case give results similar to those reported by Levitt [13].

3. Results

3.1. The polarization energy

We first study the simplest case, with only two dielectric phases. The dielectric constant of the aqueous phase is taken as $\epsilon_a = 80$, that of binding cavity $\epsilon_c = \epsilon_a$, and the dielectric constant of the protein-membrane is $\epsilon_m = 2$. The thickness of the membrane-protein is assumed to be 50 Å, and the radius of the binding cavity is 3 Å. The bound ion is a univalent cation, and the charge coordinating groups on the protein are represented by a uniform ring of charge -1, giving overall electroneutrality.

Fig. 2 shows the electrostatic potential for a point charge when the well depth is 28 Å. From a comparison of Fig. 2a and b, it is clear that the Coulombic contribution to the potential is small, and the potential pattern mainly reflects the polarization contribution. Even at the site of the ring of coordinating charge, only 2.5 Å from the cation, the polarization potential due to the cation is 25.2 RT/e (R = gas constant; T = absolute temperature, e = unit proton charge), while the cation's direct Coulombic potential at the same position is only 2.8 RT/e because of the high dielectric constant of water. The electrostatic interaction energy of the cation and the protein is thus dominated by polarization effects.

According to Eq. (3), the polarization energy of ion binding has three components: the energy of the bound ion under its own polarization field, $w_1 = (1/2)q_1\psi_{p1}(r_1)$; the energy of the ion in the polarization field of the protein charged groups, $w_2 = (1/2)q_1\psi_{p2}(r_1)$, and the energy of the protein charged groups in the polarization field of the ion, $w_3 = (1/2)q_2\psi_{p1}(r_1)$. The electrostatic reciprocity relationship requires that $w_2 = w_3$. This provides an opportunity to evaluate the numerical accuracy of our approach, since we can calculate w_2 and w_3 independently. Fig. 3 shows these components of the polarization energy for ion binding, as a function of the depth of the binding cavity. When the radius of the charged ring is 2.5 Å, there is a difference of about 10% in w_2 and w_3. This error is due to the size of the surface elements in our calculation, which are at a grid interval of 1 Å; this is too coarse to allow

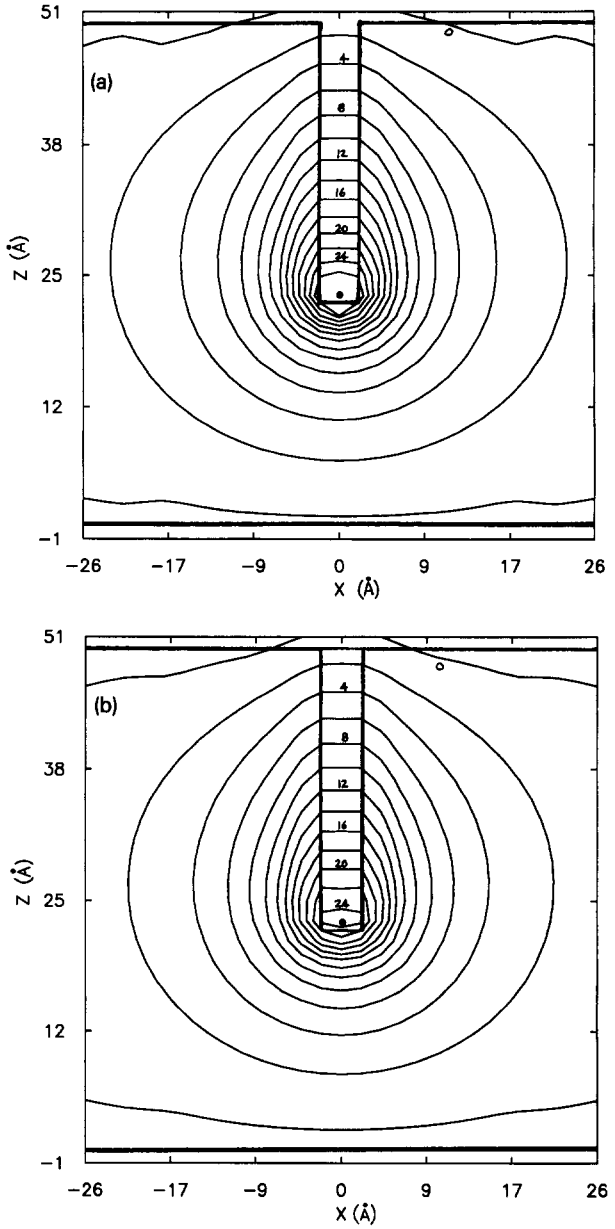

Fig. 2. Contour map of the polarization potential due to a point unit charge in an aqueous well inside a membrane. The thickness of the membrane is 50 Å, the radius of the well is 3 Å, the well depth is 28 Å, and the charge is located 1 Å above the bottom of the well. The surfaces of the membrane and well are shown by heavy lines, and the position of the fixed ion is represented by the solid circle. Distances along the two axes are measured in Å. Contours are drawn at intervals of 2 RT. (a) Total potential, which is the sum of Coulombic and polarization contributions. (b) Polarization potential alone.

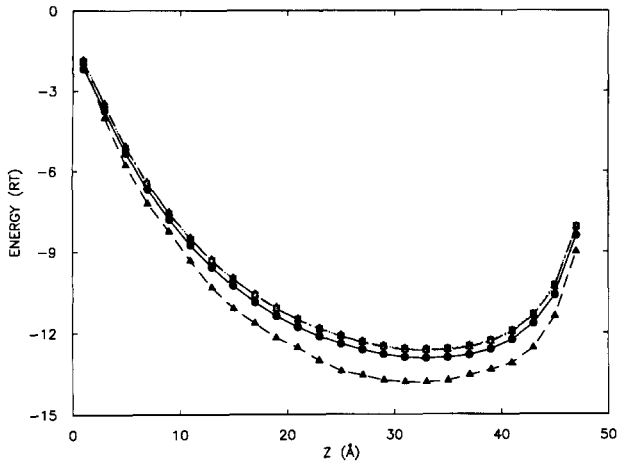

Fig. 3. Polarization energies of a point unit charge ($q = 1$) interacting with the charges of a model binding site, as a function of the depth of the well, Z. Geometry of the charge in the well is identical to that of Fig. 2. The binding site is represented by a ring of uniform charge ($q = -1$) placed concentrically about the point charge. Three energy components are shown. w_1: the interaction of the point charge with its own polarization potential; w_2: the interaction energy of the point charge with the polarization potential of the ring charge; w_3: interaction of the ring charge with the polarization potential of the point charge. w_1 is positive and independent of ring diameter; the solid circles indicate $-w_1$. Electrostatic reciprocity requires $w_2 = w_3$, so differences between these indicate the magnitude of the numerical errors in our method. Two cases are treated, one with a ring radius of 2.5 Å (w_2: solid triangles; w_3: open squares; the difference between these is about 10%), and the other with a ring radius of 2.0 Å (w_2: open triangles; w_3: open diamonds, which coincide almost exactly with the open triangles).

accurate calculation of the ring-induced polarization charge when the ring charge is only 0.5 Å from the edge of the well, so w_2 is in error. If the radius of the ring is reduced to 2.0 Å, however, the difference between w_2 and w_3 is less than 0.1% and the reciprocity relationship holds, as required.

The insensitivity of w_3 to ring size (Fig. 3) is due to the fact that the cation is far enough from the walls of the well that the 1 Å grid is sufficiently fine to accurately determine the polarization charge induced by the cation. We take advantage of the reciprocity relationship and the greater accuracy of w_3 than w_2 when calculating the contributions of polarization to the ion binding energy, which is

$$\Delta w = w_1 + w_2 + w_3 = w_1 + 2w_3$$

w_1 and w_3 are very similar in magnitude, but opposite in sign (Fig. 3), so the binding energy curve $\Delta w(Z)$ has essentially the same shape as the curve for w_3 (or $-w_1$). In the case of Fig. 3, the maximum value of $|\Delta w|$ is 12.9 RT, when the depth of the binding site is about 3/5 of the total thickness of the membrane. This energy is larger in magnitude than the energy barrier for ion transport across a membrane of similar thickness through an aqueous pore of radius 3 Å [13]. This is because removal of the ion from the binding site leaves a ring of negative charge buried in a deep well, which is a very high energy configuration. Ion binding represents the approximate neutralization of the ring charge.

The energy profile here shows a characteristic asymmetry with respect to the distance of the binding site from the surfaces of the membrane, because the well is open to only one side of the membrane. If the ion and the charged ring were located completely outside the membrane, and if the membrane is flat without any cavity, the polarization energy could be simply calculated by the image charge method:

$$\Delta w = \left(q^2/\epsilon_a\right)\left(1/(2d) - \left(r^2 + (2d)^2\right)^{-1/2}\right) \qquad (9)$$

where d is the distance of the ion to the surface of the membrane and r the radius of the ring charge with the ion located at the center of the ring. If the excluded volume requirement is met (d is larger than $2r$), then Δw will remain negative whether the complex is inside the well or outside the membrane. In our more detailed model (Fig. 3), the magnitude of the polarization energy increases monotonically as the well depth increases, until the well is deep enough that polarization effects on the other face of the membrane begin to take effect. Beyond that point, the magnitude of the polarization energy again drops. One purpose of this paper is to show the asymmetry in this curve, whose inflection point is well past the midpoint of the membrane.

The polarization energy depends on the radius of the binding cavity. Fig. 4 compares the polarization energies for ion binding in the cavity with three different well radii: 3 Å, 4 Å, and 5 Å. Again, the ion is a monovalent cation, and the binding group charge is -1. It is observed that when the channel radius increases from 3 Å to 5 Å while the thickness of the membrane remains unchanged, the magnitude of the maximum polarization energy decreases

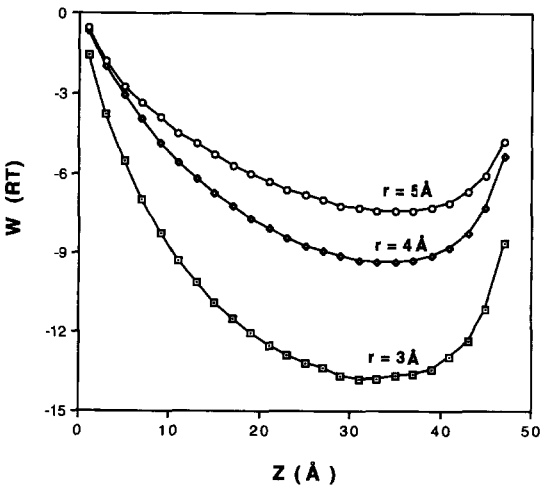

Fig. 4. Comparison of binding energies of a monovalent ion in binding wells of different radii, as a function of well depth. The thickness of the membrane is 50 Å.

from 12.9 *RT* to 7.4 *RT*. The latter would predict a binding constant of $1.6 \cdot 10^3$. Note that in all these energy profiles, similar asymmetric patterns with respect to the depth of the binding site are observed.

Since the actual structure of the membrane with transport proteins embedded inside is not a uniform flat structure, we have examined more realistic models. It has been known for some time that the SR Ca^{2+} pump embeds in the membrane in an asymmetric fashion, with a mushroom-like stalk and head on the cytoplasmic (uptake) side of the membrane. Cryo-electron microscopy has recently shown that this shape resembles the head and neck of a bird [22]. We have examined various model geometries, finding that the most important parameter is the total length of the protein; if the stalk is at least 10 Å in diameter, variations in radius and exact shape of the stalk and head have little influence, and a simple cylindrical model for the protein reproduces the energetics with small error. We have thus examined such a model in some detail.

We have chosen to model the known geometry of the stalk and transmembrane regions of the SR Ca^{2+}-ATPase [22]. We have not included the head, to allow for the possibility that the channel does not pass through the entire protein, but that the entrance is near the junction of the stalk and head. (The effects of binding site asymmetry become even greater if we consider the total height of the protein, so these calculations are a conservative estimate of the contributions of asymmetry.)

Our model consists of a cylindrical protein with one end flush with the discharge face of the membrane, while the other end protrudes 20 Å above the membrane surface on the uptake side (see the inset of Fig. 5). The inside radius of the well for ion binding is chosen to be 3 Å, and the outside radius of the cylindrical protein, *R*, is examined for three different values: $R = 5$, 10, and 20 Å. These

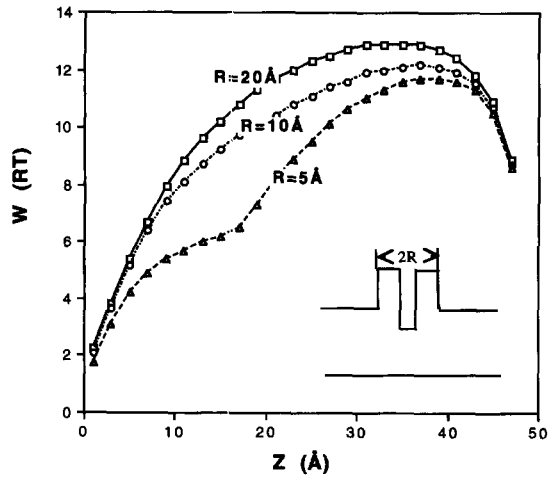

Fig. 5. Dependence of binding energy on the geometry of transport protein. The structure is shown schematically in the inset of the figure. The inner radius of the binding cavity is 3 Å, and *R* is the outside radius of the cylindrical protein. The top of the protein is 20 Å above the rest of the membrane surface. The membrane thickness is 30 Å.

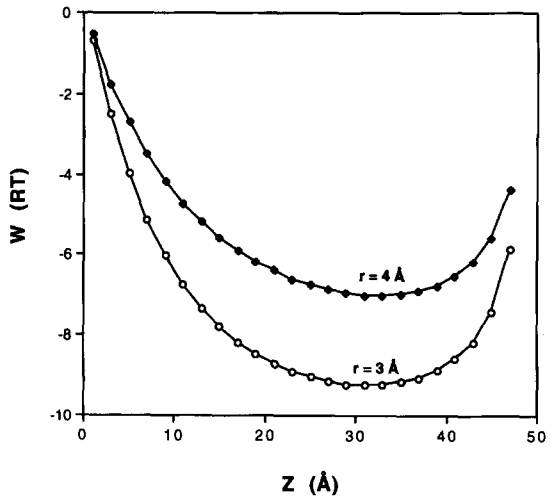

Fig. 6. Dependence of polarization binding energy on the depth of the well for the case where the dielectric constant inside the binding cavity is 40. The geometric parameters are identical to those of Fig. 2, except that two different values are considered for the radius of the binding cavity, 3 Å and 4 Å (compare to Fig. 4).

values span the range that would be appropriate for the stalk of the SR Ca^{2+}-ATPase [22]. The calculated polarization energy of a point charge, *W*, is shown as a function of the location of the binding site in Fig. 5. Compared with the results shown in Fig. 3, it is seen that if the outside radius of the protein is small (e.g., $R = 5$ Å), the variation of polarization energy with the depth of the binding site can be significantly modified. However, if *R* is larger than 10 Å, the polarization energy in such structures becomes close to that of the structures with a uniform thickness of 50 Å. In fact, when $R = 20$ Å, the two models are almost identical. It is concluded that, as long as the outside radius of the stalk portion of the transport protein is not too thin, protein protrusions on either side of the membrane simply increase the effective membrane thickness. The depth of the binding site can be taken as the distance from the site to the face of the intake channel, not the distance measured from the surface of the membrane.

Finally we consider the effect of variations in the dielectric constant inside the well. Due to the highly constrained nature of water molecules inside the channel, the dielectric constant inside the channel may be substantially smaller than that of bulk water. As a test, we have considered the dielectric constant inside the binding cavity, ϵ_c, as 40, which is between the dielectric constant of the membrane and that of bulk water. The system then consists of three dielectric domains. The calculated binding polarization energy for such a system is shown in Fig. 6. The thickness of the membrane is 50 Å. The minima of the polarization energies for $r = 3$ Å and 4 Å are -9.3 *RT* and -7.0 *RT*, respectively. It is observed that if the dielectric constant inside the cavity is reduced by 50% with respect to that of bulk water, the polarization energy drops by about 20–30%.

3.2. Difference of polarization energy between two transport states

The above calculations show the characteristic asymmetric profile of the polarization energy with respect to the binding site location in the membrane. If access to the binding site is switched from one face of the membrane to the other while the location of the charges is not changed during the conformational transition (Fig. 1), it is expected that the binding energy will jump to a different value. The energy of ATP hydrolysis would drive this transition. The difference of polarization energies between the two states determines the relative binding affinity of the ion in the uptake and discharge states. The magnitude of the polarization energy difference between the two conformations is determined by the location of the binding sites. We define h_i as the distance from the binding site to the membrane surface on the uptake side, and h_o as the distance from the binding site to the other surface of the membrane (Fig. 1). We assume that the location of the binding site is not appreciably changed during the conformational transition from the E_1 state to the E_2 state, so that $H = h_i + h_o$. The asymmetry of the two binding conformations is measured by the ratio $\lambda = h_i/H$. $\lambda = 0.5$ represents a site located equidistant from the two sides of the membrane. $\lambda > 0.5$ indicates that the site is closer to the discharge side of the membrane. The difference of polarization energy is calculated as

$$\Delta\Delta w = \Delta w(h_o) - \Delta w(h_i) \quad (10)$$

Fig. 7 shows the calculated difference of polarization energies for a monovalent cation at the binding site in the uptake and discharge conformation, as a function of the asymmetry factor λ. The total charge of the binding groups is again taken to be -1. The thickness of the protein-membrane is taken as 50 Å. We have examined different possible cases. Curves 1 and 2 in the figure are for the cases where the dielectric constant of the binding cavity is identical to that of bulk water, and the radius of the well is 3 Å and 4 Å, respectively. Curves 3 and 4 are for a dielectric constant of 40 inside the binding cavity, and the radius of the well is 3 Å and 4 Å, respectively.

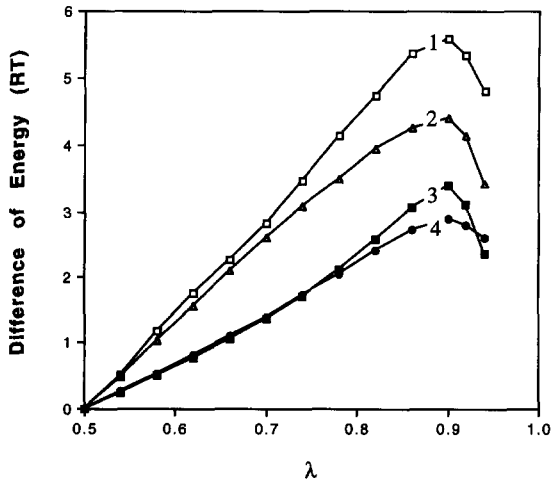

Fig. 7. The difference of polarization energy of ion binding in the two states of transport as a function of the binding site asymmetry factor, $\lambda = h_i/H$. Curves 1 and 2, dielectric constant inside binding cavity is 80, well radius is 3 Å and 4 Å, respectively. Curves 3 and 4, dielectric constant in the cavity is 40, well radius is 3 Å and 4 Å, respectively.

The results of this model show that: (1) there is a directional increase in the difference of the binding free energy with the asymmetry ratio. For $\lambda < 0.9$, the variation of $\Delta\Delta w$ with λ is nearly linear: $\Delta\Delta w = B\ (\lambda - 0.5)$, where B is a constant. For the series of curves 1 to 4 in Fig. 7, the constant B is 14.9 *RT*, 11.8 *RT*, 8.5 *RT* and 7.5 *RT*, respectively. (2) The difference of binding energy between two transport states is less dependent on the radius of the binding well than is the polarization energy of single conformations. (Compare curves 1 and 2 with Fig. 4.) For example, when $\lambda < 0.7$, $\Delta\Delta w$ changes less than 0.3 *RT* as the radius of the binding cavity increases from 3 Å to 4 Å; the binding polarization energies, on the other hand, decrease more than 3 *RT* at $Z \sim 30$ for both cases of $\epsilon_c = 40$ and 80. (3) Decreasing the dielectric constant inside the binding cavity reduces the difference of binding energy between two transport states. The maxima of the binding energy difference for curves 1 to 4 are 5.6 *RT*, 4.4 *RT*, 3.5 *RT* and 2.9 *RT*, respectively. The binding free energy difference is about 2 *RT* for a channel radius of 3 Å and $\epsilon_c = 20$, and about *RT* for the same channel radius and $\epsilon_c = 10$. (4) The binding free energy difference is somewhat less sensitive to the dielectric constant inside the well than is the binding free energy to a single site. (Compare curves 1 and 3 of Fig. 7 with the curves for $r = 3$ Å in Figs. 4 and 6.) (5) The maximum binding free energy difference is found if the binding site is very asymmetrically located, about 90% of the way through the membrane.

The above calculations have been for the case of a monovalent cation and a charge of -1 on the binding site. If we assume that the total charge of the binding groups are equal and opposite to the charge of the bound ion, i.e., the overall charge in the complex is zero, then for an ion of valence q, the difference of binding free energy would be $q^2\Delta\Delta w$, where $\Delta\Delta w$ is the binding free energy difference for a monovalent ion. This indicates that transport proteins can produce larger free energy differences by binding site asymmetry for multivalent ions than for monovalent species.

4. Discussion

The main result of these calculations is the demonstration that an asymmetric location for an ion binding site in a membrane can produce a substantial free energy difference for binding to the uptake and discharge states. Experimentally, it has been determined that the binding free

energy difference between the uptake and discharge states in the sarcoplasmic reticulum Ca^{2+}-ATPase is about 5 kcal/mol (~ 8 *RT*) [2,4,6]. ATP-driven Na^+ and K^+ pumps have similar uptake and discharge states, and the experimentally estimated binding free energy difference for the two states is about 2–4 kcal/mol (3–7 *RT*) [6]. To see how the polarization energy alone can match the observed free energy difference, consider the following example: assume that the membrane thickness is 50 Å, the radius of the binding cavity is about 3–4 Å, and the dielectric constant inside the well is identical to that of bulk water. From the results shown in Fig. 7, it is found that an asymmetry factor of 0.7 would generate a binding energy difference of 10 *RT* between the two transport states for $q = 2$. This is sufficient to account for the observed difference in binding affinities for the E_1 and E_2 states of the SR Ca^{2+} pump. For the case of the Na^+ and K^+ pumps, the experimentally observed free energy difference in the two transport conformations can be matched for a monovalent ion by an asymmetry factor of about 0.8. Even if the dielectric constant is only half that of bulk water ($\epsilon_c = 40$), the binding energy difference produced by binding site asymmetry would still be quite close to the experimentally observed values.

The sources that produce the above differences in binding affinities are similar to those that create a barrier to ion transport through ion channels, i.e., the polarization energy of the ion charge interacting with the membrane [12–14]. However, in the case of active transport, polarization energy differences are used to promote ion transport, while in the case of ion channels, the polarization produces an energy barrier to ion movement.

In the above calculations, the positions of the bound ion and the coordinating charged groups on the protein are assumed not to change as the protein moves from the uptake to the discharge conformation. This assumption allows us to calculate the free energy difference available from electrostatic asymmetry alone. We do not mean to imply, however, that polarization energies alone determine the binding affinities in active transport. Specific binding interactions must, of course, be involved in allowing active transport systems to discriminate between different ions. Changes in these interactions could also be important for the transport process [6]. Clearly, both binding site asymmetry and changes in coordination geometry might play roles in active transport.

As mentioned in the introduction and reviewed by Läuger [3], there are two classes of models for active transport, based on whether the conductance and dielectric constant of the entrance channel are high, like water at physiological ionic strength (low field models), or whether they are low, like lipids and proteins (high field models). Our model lies between these extremes. By varying the width and dielectric constant of the access channel, our model can be shifted toward the low or high field models. Our investigations are aimed at a different issue, however, namely determining the possible contribution of the polarization energy to the difference in binding constants between the uptake and discharge conformations. We find that this contribution is maximized in a narrow channel (which is like high field models) and when the dielectric constant in the channel is high (which is like low field models).

There is one significant experimentally testable prediction that follows from this work: if polarization effects are indeed a major factor in the efficient coupling of ATP hydrolysis to active transport, the uptake channel must be considerably deeper than the discharge channel. When the three dimensional structure of a transmembrane pump is finally determined at atomic resolution, detailed electrostatic calculations using standard methods [25–28] can be used to more accurately determine the contributions of polarization effects to binding free energy differences. Such calculations would also allow the possible genetic engineering of pumps with altered properties. In this regard, it has recently been shown that such design efforts can actually increase the activity of a 'perfect' enzyme whose reaction rate was known to be diffusion limited [30].

MacLennan [18] has reported that, in the calcium ATPase of sarcoplasmic reticulum, the sites of high affinity calcium binding are located in the center of the transmembrane domain. This molecule has a large headpiece protruding into the cytoplasm on the uptake side [1,18,22]. A similar structure is observed for the plasma membrane calcium ATPase [19]. Thus, the uptake channel may be much deeper than the discharge channel. If so, electrostatic asymmetry could play an important role in the rate of transport. We would suggest that such asymmetry may be a common, if not universal, feature for electrogenic ion transport systems.

Acknowledgements

This study was supported by a grant from the National Institutes of Health (2P01-HL34343).

References

[1] Inesi, G. (1985) Annu. Rev. Physiol. 47, 573–601.
[2] Schatzmann, H.J. (1989) Annu. Rev. Physiol. 51, 473–485.
[3] Läuger, P. (1991) Electrogenic Ion Pumps, Sinauer Associates, Sunderland.
[4] Tanford, C. (1983) Annu. Rev. Biochem. 45, 379–409.
[5] Stein, W.D. (1986) Transport and Diffusion Across Cell Membranes, Academic Press, Orlando.
[6] Tanford, C. (1982) Proc. Natl. Acad. Sci. USA 79, 2882–2884.
[7] Patlak, C.S. (1957) Bull. Math. Biophys. 19, 209–235.
[8] Vidaver, G.A. (1966) J. Theor. Biol. 10, 301–306.
[9] Jardetzky, O. (1966) Nature 211, 969–970.
[10] Harvey, S.C. (1989) Proteins 5, 78–92.
[11] Honig, B., Hubbell, W. and Flewelling, R. (1986) Annu. Rev. Biophys. Biophys. Chem. 15, 163–193.

[12] Parsegian, A. (1969) Nature 221, 844–846.
[13] Levitt, D.G. (1978) Biophys. J. 22, 209–219.
[14] Jordan, P.C. (1982) Biophys. J. 39, 175–164.
[15] Nakao, M. and Gadsby, D.C. (1986) Nature 323, 628–630.
[16] Nakao, M. and Gadsby, D.C. (1989) J. Gen. Physiol. 94, 539–565.
[17] Rakowski, R.F., Vasilets, L.A., LaTona, J. and Schwartz, W. (1991) J. Membr. Biol. 121, 171–187.
[18] MacLennan, D.H. (1990) Biophys. J. 58, 1355–1365.
[19] Carafoli, E. (1992) J. Biol. Chem. 267, 2115–2118.
[20] Clarke, D.M., Loo, T.W., Inesi, G. and MacLennan, D.H. (1989) Nature 339, 476–478.
[21] Asturias, F.J. and Blasie, J.K. (1991) Biophys. J. 59, 488–502.
[22] Toyoshima, C., Sasabe, H. and Stokes, D.L. (1993) Nature 362, 469–471.
[23] Jackson, J.D. (1975) Classic Electrodynamics, 2nd Edn., John Wiley and Sons, New York.
[24] Kirkwood, J.G. (1934) J. Chem. Phys. 2, 351–361.
[25] Gilson, M.K., Sharp, K. and Honig, B. (1987) J. Comp. Chem. 9, 327–335.
[26] Gilson, M.K. and Honig, B. (1988) Proteins 4, 7–18.
[27] Sharp, K.A. and Honig, B. (1990) Annu. Rev. Biophys. Biophys. Chem. 19, 301–332.
[28] You, T.J. and Harvey, S.C. (1993) J. Comp. Chem. 14, 484–501.
[29] Luchka, A.Y. (1965) The Method of Averaging Functional Corrections: Theory and Applications, Academic Press, New York.
[30] Getzoff, E.D., Cabelli, D.E., Fisher, C.L., Parge, H.E., Viezzoli, M.S., Banci, L. and Hallewell, R.A. (1992) Nature 358, 347–351.